Energy Equip. Sys./ Vol. 10/No. 4/Dec. 2022/ 401-415

ENERGY EQUIPSYS

Energy Equipment and Systems

http://energyequipsys.ut.ac.ir
www.energyequipsys.com

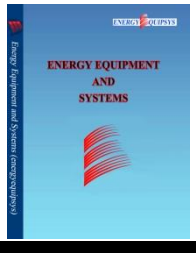

Numerical modeling of particles resuspension due to human stepping

Authors

Behrang Sajadi[a*]
Mohammad Hassan Saidi[b]
Goodarz Ahmadi[c*]
Mohsen Soleimani[a]

[a] School of Mechanical Engineering, College of Engineering, University of Tehran, Tehran, Iran

[b] School of Mechanical Engineering, Sharif University of Technology, Tehran, Iran

[c] Department of Mechanical & Aeronautical Engineering, Clarkson University, Potsdam, NY, USA

Article history:

Received : 11 December 2021
Accepted : 1 February 2022

ABSTRACT

In this paper, the induced airflow and the resultant resuspension of particles due to human walking are studied numerically using the dynamic mesh technique. Based on the results, the air is ejected from the sole and floor gap when the foot moves down, similar to a radial wall jet. During the upward motion, a strong gap flow is induced beneath the sole, which causes the surrounding air to be sucked toward the shoe center. Accordingly, particles are mainly detached in the downward motion of the foot. Then, they are entrained into the far-field flow during the foot's upward motion. Simulations indicate that the region beneath the sole edges is the most susceptible area for particles to be detached. As a result, fast walking is associated with a higher resuspension rate per footstep, up to two orders of magnitude due to increased shear stress on the floor. Although the shoe size influences the rate of particle resuspension, it is not as significant as the stepping time. Based on the results, the shear velocity due to stepping may be up to 0.4 m/s which can resuspend 10 μm particles with a resuspension rate of about 10^{-5} s^{-1}. The effect of the main geometric features of the stepping process, including the stepping time and the shoe size, are investigated to provide a general correlation for its prediction with the R-squared value of 0.99.

Keywords: Particles Resuspension, Walking, Computational Fluid Dynamics, Dynamic Mesh.

1. Introduction

In recent decades, indoor air quality (IAQ) and particulate matter (PM) exposure have become increasingly attractive among researchers worldwide. It has been shown that PM mass concentration is often higher in indoor environments than outdoors [1]. As people spend most of their time indoors [2], investigating indoor PM sources is essential to understand how occupants may be exposed to particulate matter. The highest mass loadings of particles in residences are usually found in mattresses, upholstered furniture, and floorings usually littered with microorganisms such as viruses, bacteria, and fungi [3]. These particles may be easily resuspended due to occupants' activities and become a threat to the occupants [4]. As reported by Qian and Ferro [5], human walking increases the indoor concentration of

* Corresponding authors:
Behrang Sajadi
School of Mechanical Engineering, College of Engineering, University of Tehran, Tehran, Iran
Email: bsajadi@ut.ac.ir
Goodarz Ahmadi
Department of Mechanical & Aeronautical Engineering, Clarkson University, Potsdam, NY, USA
Email: gahmadi@clarkson.edu

PM considerably; Thatcher and Layton [6] showed this increase to be up to 100%. The resuspension effect is significant for particles in the range of 5-10 μm [7]. However, sub-micrometer particles have also been shown to resuspend from normal human walking [5]. Understanding the airflow and particle resuspension due to human activities, such as walking, can provide important insight into how such activities increase PM concentration in indoor environments.

The shoe has been modeled as a disk in several previous studies to simplify the complicated process of walking. Khalifa and Elhadidi [8] studied the unsteady airflow and the particle detachment caused by a descending falling disk. Their results showed that the particle detachment mechanism is mainly due to a high-speed radial wall jet formed between the disk and the floor. Besides, the disk motion generates axisymmetric vortices at its tip, which shed after impacting the floor. These ring vortices have no significant effect on the resuspension of particles. However, their contribution to the dispersion of detached particles is considerable. These results are generally supported by Kubota et al. [9], who investigated the induced airflow due to a stomping disk using a particle image velocimetry (PIV) experimental technique. They also concluded that it is much more difficult to resuspend particles close to the disk center than close to its perimeter. Zhang et al. [10] developed a model to predict particle detachment, resuspension, and transport due to the occupants walking, which accounts for the particle adhesion force. Although they considered the stepping process an up-and-down motion using a simple two-disk model, their semi-analytical solution predicted the particle resuspension rate with acceptable accuracy. Oberoi et al. [11] studied the short-term resuspension of particles from carpets caused by the walking of an occupant using the immersed boundary method and Eulerian description of the particulate phase. They considered the carpet a porous medium and assumed that the particle adhesive force per unit mass is inversely proportional to the particle diameter squared. Their results showed good agreement with the experimental data. However, investigation of the airflow details induced by the stepping process and the description of the behavior of particles through Lagrangian trajectory analysis has considerable advantages for understanding the effect of walking on the resuspension and dispersion of particulate matter in indoor environments.

Kubota and Higuchi [12] carried out an experimental study to model the particle resuspension and dispersion due to upward and downward foot motions. They showed that the three-dimensional vortex dynamics affect particle redistribution's strength. In another study conducted by Goldasteh et al. [13], a moving shoe was modeled throughout a gate cycle. Their findings indicated that the contribution of the shoe front side in the particle resuspension is more considerable than its lateral side. Tian et al. [14] studied indoor relative humidity's effect on the particle resuspension rate. They observed a direct relationship between the relative humidity and the resuspension rate for the cut pile carpet. At the same time, there was an inverse relationship for the hard flooring. Qian et al. [15] conducted an extensive review regarding the resuspension of particles due to walking. However, they did not find a perfectly understandable answer for the resuspension mechanism and its affecting factors. Khare and Marr [16] measured the velocity of the resuspended particles using a sonic anemometer. They concluded that the taller the people are, the less exposed to the resuspended particles. In their work, Han et al. [17] analyzed how human movement can affect pollutant distribution and concentration as a result of aerodynamic effects and induced wake, both experimentally and numerically. In 2017, Benabed and Limam [18] exploited a setup equipped with an optical particle counter. They investigated the behavior of particles using a plate of rectangular shape, which can mimic the foot rotation during stepping down. Their experiments showed that particles with a diameter of 1-10 μm have more considerable resuspension source strength than particles with less than 1 μm. Besides, a rough surface is associated with higher particle resuspension than a smooth floor. Different shoe and flooring types were also investigated in experimental research work by Lai et al. [19], indicating that carpet flooring is associated with higher resuspension than tile. In 2020, Wang et al. [20]

studied experimentally, as well as numerically, the effect of occupants walking on $PM_{2.5}$ suspension in a typical classroom during a multi-day period. Their results support the importance of walking on the resuspension of particles. More recently, Zhang and Yao [21] conducted a similar research work on the effect of children walking on the resuspension of biological particles. They used a robot for their experiments to study the impact of shoe materials on the resuspension increase ratio (RIR). They reported higher resuspension of large particles than sub-micron ones. Besides, according to their results, walking with cotton socks resuspend more particles than PVC and EVA shoes.

Although there are some previous research works regarding particle resuspension due to stepping, there is still a lack of knowledge about the physical concepts of the resuspension process. Besides, the effect of stepping features, especially the stepping time as a criterion for walking speed, has not been assessed yet. In this research, the induced airflow and the resultant detachment of particles caused by the stepping process are studied numerically using a detailed model, which includes all the geometric and physical features of actual walking. Simulation of the resuspension of particles includes a model that uses the particle-surface adhesion force for predicting the critical shear velocity or shear stress that causes the particles to detach from the floor. The simulation results provide better insight into the resuspension of particles during human walking and, consequently, the increase of PM levels in indoor environments.

2. Numerical Modeling

Figure 1 shows the basic model for which specifications are summarized in Table 1. Grid sensitivity studies showed that an 8×10^5 non-uniform tetrahedral initial mesh guarantees the independence of the simulation results from the number of grids.

For an unsteady incompressible flow, the governing equations are:

$$\rho\frac{\partial\phi}{\partial t}+\nabla.(\rho\boldsymbol{V}\phi-\Gamma_\phi\nabla\phi)=S_\phi \quad (1)$$

where $\mathbf{V}$ is the velocity vector and the effective diffusion coefficient, Γ_ϕ, and the source term, S_ϕ, for different parameters, ϕ, are listed in Table 2.

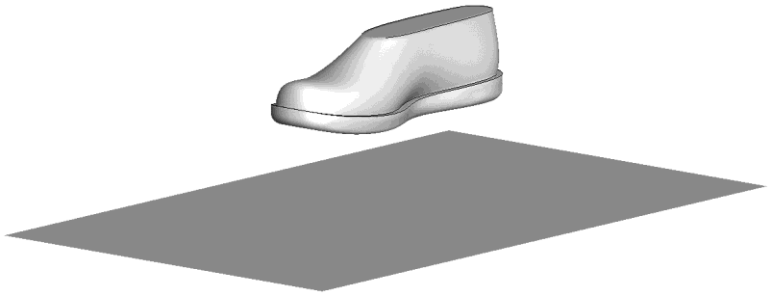

(a) Geometry of the modeled shoe

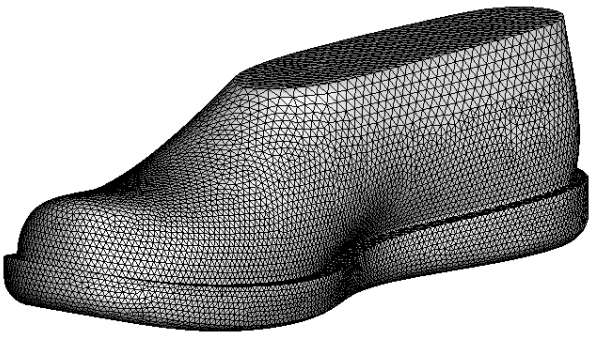

(b) The generated mesh of the modeled shoe

Fig. 1. The basic model

Table 1. Specifications of the basic model

Item	Value
Chamber dimensions	0.6 m × 0.4 m × 0.6 m
Shoe length	0.3 m
Sole area	0.026 m^2
Initial distance of the shoe from the floor	0.085 m
Stepping time	1.5 sec

Table 2. Coefficients and source terms of the flow governing equations

Equation	ϕ	Γ_ϕ	S_ϕ
Continuity	1	-	-
Momentum	V	μ_{eff}	$-\nabla p$
Turbulent kinetic energy	k	μ_{eff} / σ_k	$P_k-\rho\varepsilon$
Turbulent kinetic energy dissipation rate	ε	$\mu_{eff} / \sigma_\varepsilon$	$\varepsilon(C_1P_k-C_2\varepsilon) / k$

The RNG k-ε model [22], accompanied by the standard wall function [23], is implemented to resolve the turbulence closure problem due to its simplicity, robustness, and relatively accurate results [24]. The governing equations are solved on a collocated grid using ANSYS FLUENT 12.1 [25] commercial code. The dynamic mesh technique is used to update the model geometry and its computational grid in each time step. Pressure-velocity coupling is established through the SIMPLE algorithm [26], and temporal and special terms are discretized using the first-order and the second-order schemes, respectively.

As the size of studied particles is relatively large, Brownian motion is negligible, and the particle equation of motion is given as [27]

$$\frac{du_i^p}{dt} = \frac{1}{\tau}(u_i - u_i^p) + g_i \tag{2}$$

where u^p is the particle velocity, g_i is the acceleration of gravity, and τ is the particle relaxation time defined as

$$\tau = \frac{Sd^2C}{18\nu} \tag{3}$$

where d is the particle diameter, S is the particle-to-fluid density ratio and the Cunningham correction factor, C, is included to account for non-continuum effects. Thus,

$$C = 1 + Kn\left[1.257 + 0.4\exp\left(-\frac{1.1}{Kn}\right)\right] \tag{4}$$

where Knudsen number, Kn, is given as

$$Kn = \frac{2\lambda}{d} \tag{5}$$

where λ is the air mean free path, which equals 68 nm at the normal atmospheric conditions.

Other forces (such as the Saffman's lift force), which are small, are neglected.

Turbulence fluctuations strongly affect particle transport in indoor airflows and should be appropriately estimated. In this study, the discrete random walk (DRW) model is used to simulate the instantaneous turbulent fluctuation velocity components as:

$$u_i' = G\sqrt{\overline{u_i'^2}} \tag{6}$$

where G is a Gaussian random number and $\sqrt{\overline{u_i'^2}}$ is the root mean square (RMS) of the i^{th} fluctuation velocity component. For the k-ε turbulence models, the mean square of all fluctuation velocity components equals 2/3 k.

The random number, G, is updated using the eddy lifetime and the particle crossing time concepts. The characteristic lifetime of turbulence eddies may be estimated as:

$$\tau_e = 2T_L \tag{7}$$

where T_L is the turbulent Lagrangian time scale and for the k-ε turbulence models is given as:

$$T_L = 0.15\frac{k}{\varepsilon} \tag{8}$$

The particle crossing time - the time a particle needs to pass across an eddy - equals:

$$\tau_C = -\tau \ln\left(1 - \frac{L_e}{\tau\left|u - u_p\right|}\right) \tag{9}$$

where L_e is the eddy length scale and $\left|u - u^p\right|$ is the particle's relative slip velocity magnitude. Particles are assumed to interact with a turbulence eddy over the smaller value of τ_e and τ_c. Therefore, the random number G is updated after the minimum of τ_e and τ_c.

Modified Johnson-Kendall-Roberts (JKR) theory [28] is used to simulate particle detachment due to airflow. By a user-defined function (UDF), the effect of surface energy and elastic deformation of particles are taken into account. Previous studies showed that the pull-off force on the real surfaces is lower than the original JKR model prediction due to neglecting the effect of surface roughness [29]. The analysis of Johnson et al. [28] regarding the contact of elastic spheres in the presence of adhesive force was extended to individual asperities by Fuller and Tabor [30]. They assumed that all asperities have the same radius, and their height is normally distributed. Based on Fuller and Tabor's research work, Soltani and Ahmadi [31] developed an analytical expression for predicting the particle pull-off force from rough surfaces. Accordingly:

$$F_{po} = \pi a^2 N f_{po} \exp\left[-\frac{0.6}{\Delta_c^2}\right] \text{ and} \tag{10}$$

$$a = \frac{\pi}{2K} N f_{po} d \exp\left[-\frac{0.6}{\Delta_c^2}\right] \tag{11}$$

where K is the composite Young's modulus of the particle-surface materials, and N is the number of asperities per unit area. Also, f_{po} is the pull-off force for an individual asperity contact, which is given by

$$f_{po} = \frac{3}{2}\pi W_A \beta \tag{12}$$

where W_A is the thermodynamic work of adhesion, which depends on the particle-surface materials, and β is the asperity radius assumed to be given as

$$\beta = 0.02d \tag{13}$$

Δ_c is the non-dimensional roughness parameter defined as

$$\Delta_c = \frac{\delta_c}{\sigma} \tag{14}$$

where σ is the standard deviation of the roughness height distribution, and δ_c is the maximum extension of an asperity tip above its undeformed height before the adhesion breaks. Based on the JKR theory

$$\delta_c = \left[\frac{f_{po}^2}{3K^2\beta}\right]^{1/3} \tag{15}$$

Topographical data for real surfaces presented by Greenwood and Williamson [30] showed that σ, β, and N might be well correlated by

$$\beta\sigma N = 0.1 \tag{16}$$

Soltani and Ahmadi [29, 31] noted that rolling is the most likely mechanism to detach spherical particles. Figure 2 shows the geometric features of a spherical particle attached to a rough surface. F_{po} is the particle pull-off force, and F_t and M_t are, respectively, the total external force and the total external moment induced by the flow. Gravity and Saffman's lift forces have a negligible influence on the detachment of particles of human health interest (10 micrometers in diameter and smaller) from rough surfaces [31]. So, they are not included in the analysis.

Previous experimental and numerical works showed that near-wall coherent vortices play an essential role in the resuspension of particles. Fan and Ahmadi [33] developed an analytical expression for the near-wall fluctuation flow field using a stagnation point flow model. According to their sublayer model,

$$F_t = \frac{2.9\pi\rho u^{*2} d^2}{C} \text{ and} \tag{17}$$

$$M_t = \frac{1.07\pi\rho u^{*2} d^3}{C} \tag{18}$$

where u^* is the wall shear velocity, and C is Cunningham's correction factor.

Applying a moment balance over the point "O" in Fig. 2, the critical shear velocity for the one-set of rolling is given as [31]

$$u_c^* = \left[\frac{Ca^3 N f_{po} \exp\left(-0.6/\Delta_c^2\right)}{2.52\rho d^3}\right]^{1/2} \tag{19}$$

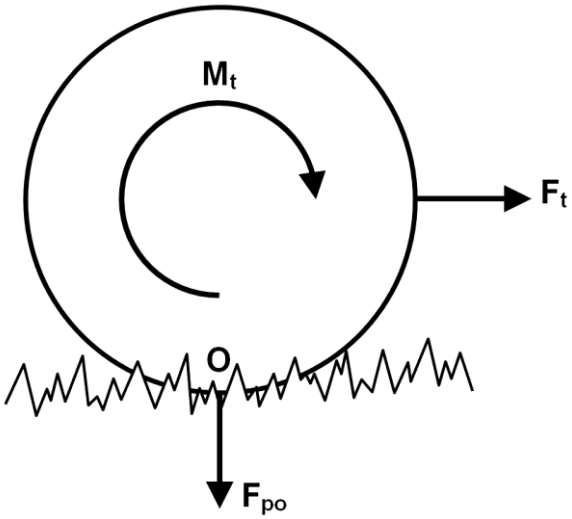

Fig. 2. Forces acting on a particle attached to a rough surface

3. Results and Discussions

Figures 3 and 4 show the velocity vectors and the vorticity magnitude contours, respectively, for different time snapshots. The induced airflow pattern may be better described by dividing the stepping process into two stages, the foot's upward and downward motions. At first, the foot is stationary, and the surrounding air is at rest. As the heel starts moving down towards the floor, a ring-like vortex is generated and grows at its tip. At the same time, the air is ejected outwards from the sole and floor gap, similar to a radial wall jet. When the heel gets close to the floor, the foot turns on the heel, and the toe starts moving downward. So, a vortex is induced on the toe tip, which has features similar to the heel vortex. However, the induced airflow caused by the downward toe motion is more powerful, making this stage susceptible to particle resuspension from the floor. The foot turns on the toe as the sole touches the floor, and the shoe starts upward. Due to the foot's upward motion, a strong gap flow is induced beneath the sole, which causes the surrounding air to be sucked toward the center of the shoe. The induced flow patterns are similar to the airflow induced by a moving disk, studied experimentally by Kubota et al. [9]. However, the airflow is asymmetric in this case, making it more complicated to describe.

The detachment of particles from the floor due to the stepping process is studied using the numerical approach discussed in the modeling section. The utilization of Arizona Test Dust (ATD), which mainly contains silicon dioxide (SiO_2) and aluminum oxide (Al_2O_3), is typical for studying the resuspension of particles in indoor environments [34]. Table 3 summarizes the specifications of SiO_2 and Al_2O_3 particles in contact with a vinyl floor [10]. Based on Eq. (19), Fig. 5 shows the effect of the surface roughness parameter and particle material on the critical shear velocity for particle detachment from a vinyl floor. As shown in Fig. 5, the behavior of SiO_2 and Al_2O_3 particles are almost the same. However, silicon dioxide particles are resuspended under slightly smaller shear velocities due to their lower work of adhesion. Consequently, as silicon dioxide approximately forms 70% of Arizona Test Dust, only SiO_2 particles are considered in the following discussions. According to Fig. 5, the critical shear velocity reduces rapidly as the particle size or surface roughness increases. As a result, the resuspension of coarse particles is much higher than that of fine particles. Particles larger than 10 μm have high deposition rates in the indoor environment and the respiratory system's upper (nasal-pharyngeal) portion. Therefore, have a relatively small contribution to the PM exposure of concern for occupants. This observation is in agreement with previous studies [7].

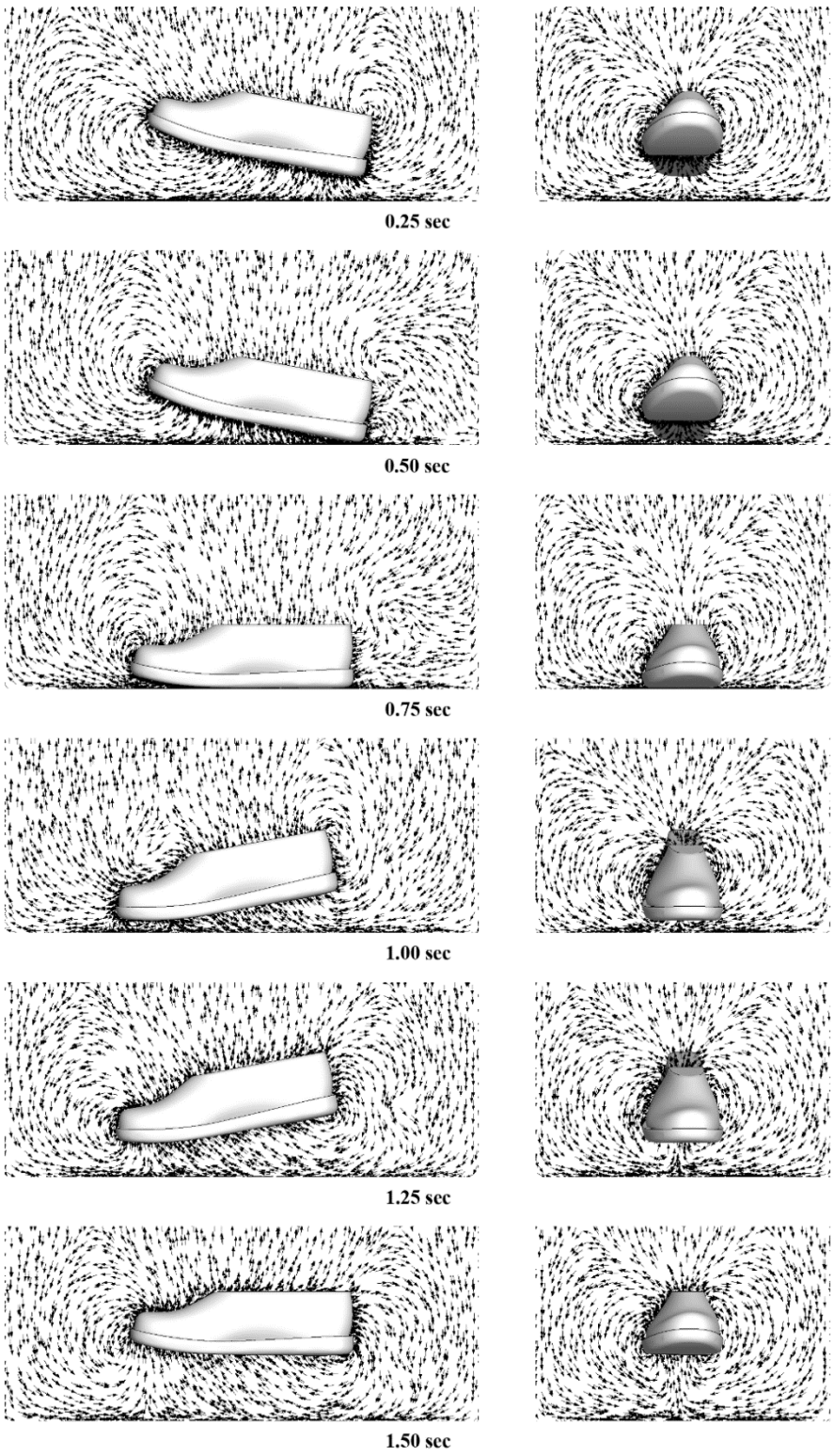

Fig. 3. Velocity vectors of the airflow induced by the stepping process

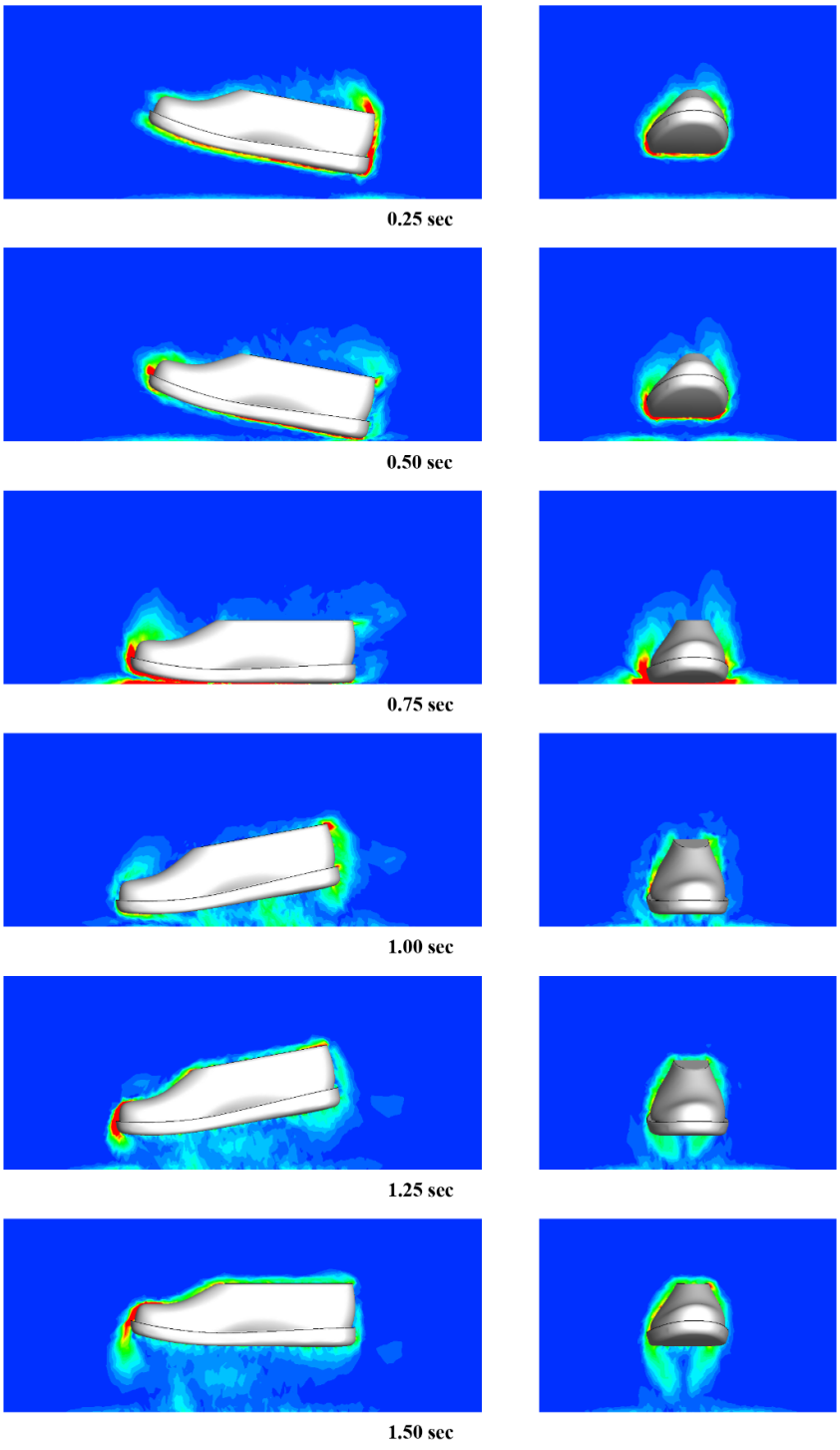

Fig. 4. Vorticity contours of the airflow induced by the stepping process

Table 3. Specifications of SiO_2 and Al_2O_3 particles in contact with vinyl floors

Material	W_A (10^{-3} J/m)	K (10^{10} N/m^2)	ρ (10^3 kg/m^3)
SiO_2	10.7	7.3	2.20
Al_2O_3	15.3	36	3.96

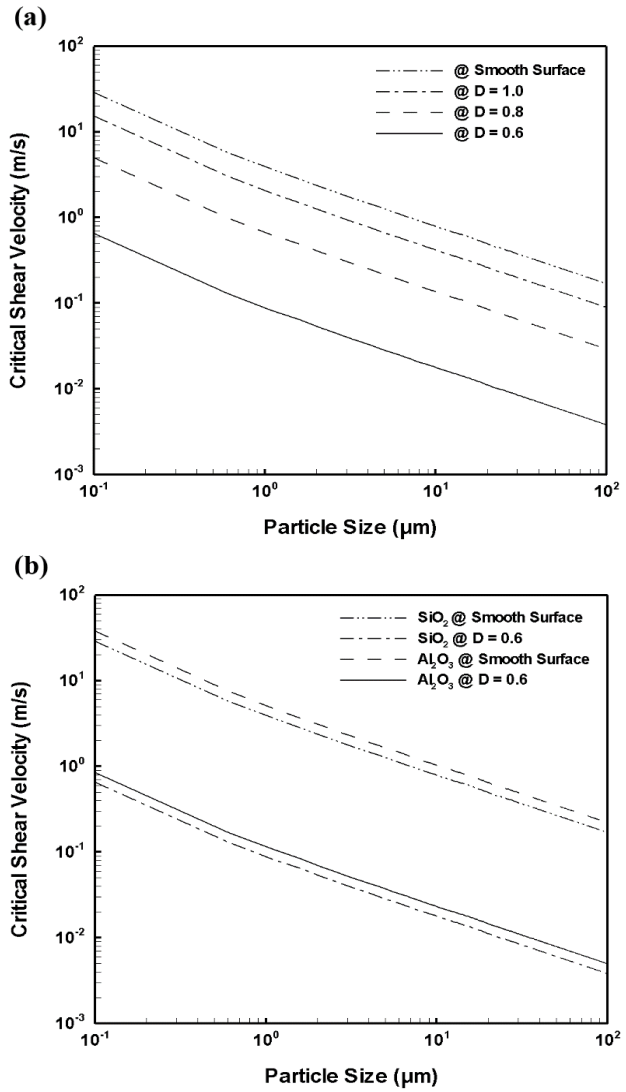

Fig. 5. The effect of main parameters on the critical shear velocity for particle resuspension

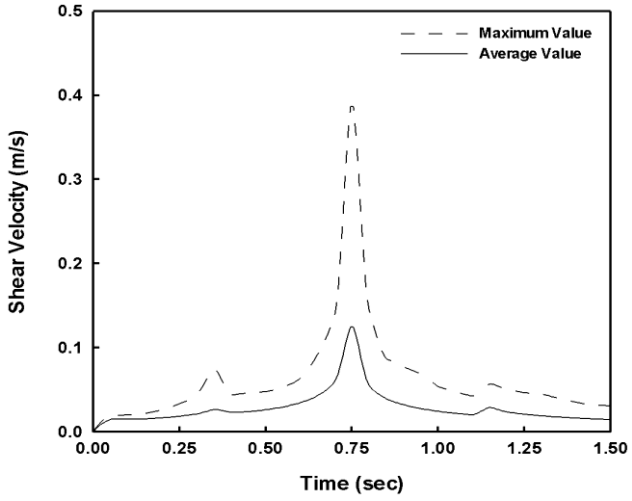

Fig. 6. Maximum and average shear velocity on the floor induced by the stepping process

As the wall shear velocity is the dominant factor in the determination of particle detachment, the variation of maximum and average shear velocities on the floor are shown in Fig. 6 during the stepping process. As depicted in the figure, the shear stress increases moderately when the foot moves down toward the floor. However, as the sole gets close to the floor, the shear stress increases sharply, supporting this stage's susceptibility to the detachment of particles. The shear stress then falls rapidly as the foot starts moving upward. As a result, the upward motion of a shoe has no significant contribution to the detachment of particles due to hydrodynamic effects. However, it is essential to entrain the resuspended particles into the far-field airflow. Two small peaks detectable in the variation of shear velocity are related to when the heel touches the floor, and the toe is detached from the floor in the upward motion. Comparing Fig. 6 with the critical shear velocity in Fig. 5, the capability of the induced airflow in detaching particles increases significantly as the sole gets close to the floor. As the foot starts upward motion, the minimum size of detachable particles increases rapidly, which is evidence of reducing the airflow potential to resuspend fine particles. The maximum shear velocity on the floor occurs near the sole edges. Therefore, this region is the most susceptible zone for particle detachment. Based on the results, sub-micrometer particles are not easily detached by the airflow induced in the studied stepping process.

The resuspension and deposition rate are used to study the stepping process effect on the behavior of the particles:

$$RR = \frac{R}{L} \tag{20}$$

$$DR = \frac{D}{L} \tag{21}$$

where R and D are the particle's resuspension and deposition fluxes, respectively, and L is the particles loading over the floor.

Figure 7 compares the numerical prediction of the resuspension rate in eight different cases with the upper and lower bands of Qian and Ferro [5] experiments for the resuspension of 5-10 μm ATD particles. Qian and Ferro [5] performed their measurements in a controlled environment, which makes the comparison of the numerical results with their data more reliable among available experimental resuspension studies. However, as it is not possible to directly measure the resuspension rate experimentally, Qian and Ferro [5] used a mass balance approach to estimate resuspension rates, and some error was introduced by assuming a well-mixed chamber [5]. Although the numerical simulations cover a relatively wide range of stepping times and shoe sizes encountered in real situations, the results agree with the experimental limits. As seen in Fig. 7, the numerical results are close to the upper limit of the experimental data, which may be because the numerical prediction of the resuspension rate of particles is based on one stepping cycle. In real conditions, the resuspension rate usually decreases with time because of the harvesting effect, making the average resuspension rate decline even up to one order of magnitude [34]. It should be noted that some factors that contributed to the resuspension of particles were not controlled in the experiments nor modeled in the simulations, e.g., person-to-person variability, walking style, and shoe type.

In the following discussion regarding particle resuspension and dispersion, 10 μm particles are considered the example particle size. Also, the non-dimensional roughness parameter is assumed to be 0.8, a reasonable value for common surfaces [10, 31]. Our previous study showed that the particle size and the surface roughness significantly affect the maximum rate of particle resuspension; however, they have no remarkable influence on its trend [35]. Accordingly, for rougher surfaces, which are represented by a larger roughness parameter, and for larger particles, which have less critical shear velocity, the resuspension of particles is higher and occurs over a more extended period.

The variation of resuspension and deposition rates of 10 μm particles during the stepping process is presented in Fig. 8. The figure shows that the particle resuspension increases rapidly as the sole gets very close to the floor. After the sole impacts the floor and the foot starts moving upward, the detachment of particles falls rapidly to almost zero.

Besides, when the shoe heel touches the floor at 0.40 seconds, a few particles are detached from the floor, causing a slight fluctuation in the variation of resuspension rate. This fluctuation is detectable in the enlarged left-lower part of the abovementioned figure. As shown in Fig. 8, there appears to be a correlation between particle deposition and resuspension rates. This trend is mainly because, for this simulation, resuspension is the only source of particles. As a result, the number of deposited particles is directly related to the resuspended particle concentration. However, there is a slight lag between the times when the maximum resuspension and deposition rates occur. This lag is mainly due to the particles' inertia effect, which prevents them from following the airflow immediately.

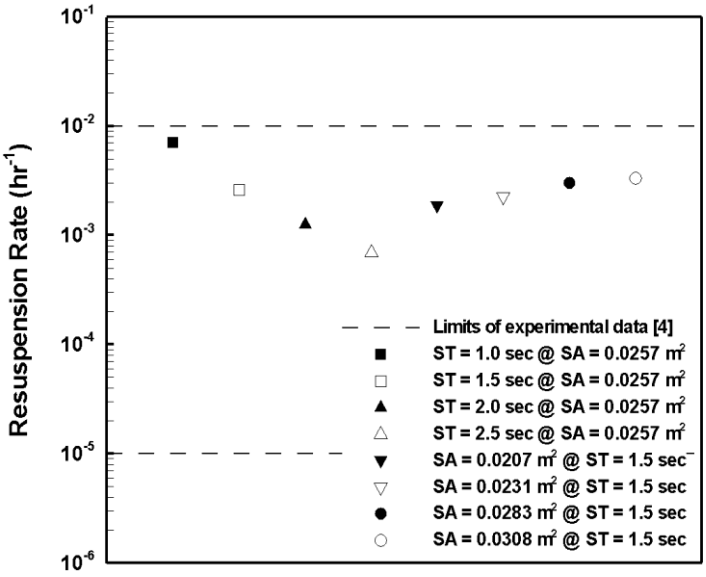

Fig. 7. Comparison of the numerical simulations with the bands of experimental data

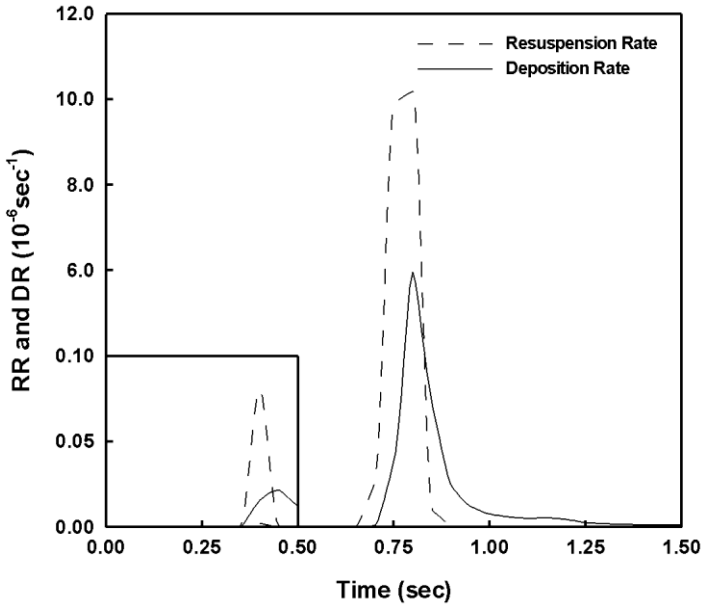

Fig 8. The rates of resuspension and deposition of 10 μm particles due to the stepping process

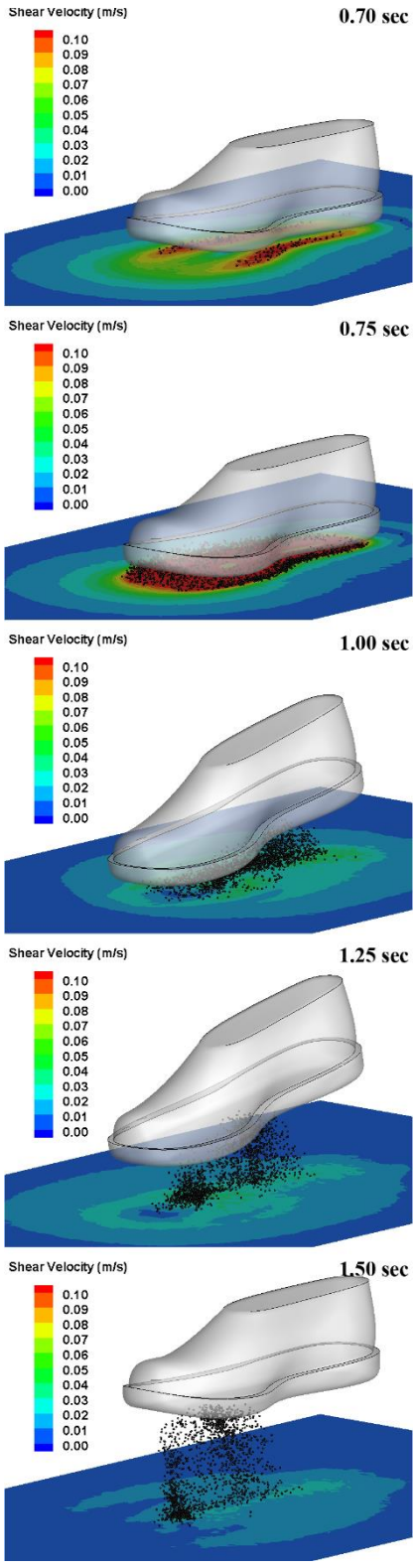

Fig. 9. Shear velocity on the floor and the resultant particles resuspension due to the stepping process

To gain better insight into the effect of the induced airflow on the dispersion of resuspended particles, a sequence of snapshots from the distribution of particles is shown in Fig. 9. The contours of shear velocity on the floor are also depicted in the figure. The snapshots are presented only after 0.70 seconds when the resuspension of particles becomes significant. Particles are resuspended near the sole edges where the shear velocity is maximal. From 0.70 to 0.75 seconds, the shear stress on the floor rapidly increases as the sole touches the floor, and most of the resuspension of particles occurs during this period. During the upwards motion of the foot, the shear velocity falls rapidly, which is evidence of the reduced potential to detach particles. In this stage, the resuspended particles are entrained into the induced gap flow and concentrate near the shoe centerline, mainly at its toe portion. As a result, the downward motion of the foot mainly contributes to the detachment of particles, and the upward motion causes the resuspended particles to disperse and entrain in the far-field airflow. There is some instability in the dispersion of particles, which is mainly attributed to the azimuthal instabilities in the ring-like vortex structure. Such instabilities have also been reported beneath falling disks[35], moving disks [12], and impacting spheres [36].

The main parameters which affect the airflow induced by the stepping process include the stepping time and the shoe size. The simulation results indicate that although the general trend of the particle resuspension rate variations during the stepping cycle is similar to Fig. 8 in all cases, the resuspension rate highly depends on these parameters. Figure 10 shows the effect of the stepping time and the shoe size on the resuspension rate. The figure shows that fast walking leads to a higher resuspension rate than less active walking, mainly due to increased shear stress on the floor. Besides, although the shoe size also influences the resuspension rate of particles, the effect is not as significant as that for the stepping time. As a general conclusion, the resuspension rate of particles increases exponentially when the stepping time gets shorter. At the same time, it depends linearly on the shoe size. This result may be better quantified using the following empirical formula, which can correlate the results with the R-squared value of 0.99,

$$RR = 2.60\times10^{-3}\left[0.98\left(\frac{ST}{1.5}\right)^{-2.52}\right]\left[1.40\left(\frac{SA}{0.0257}\right)+0.39\right] \tag{22}$$

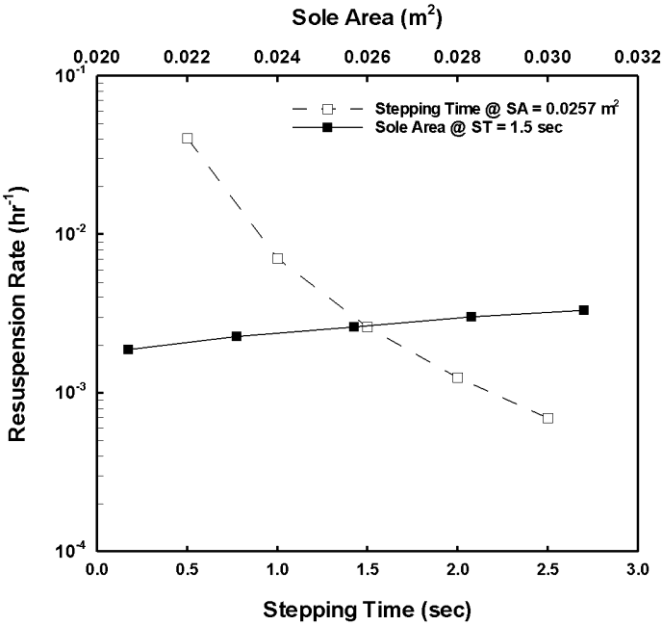

Fig. 10. The effect of the stepping time and the shoe size on the particles resuspension rate

4. Conclusions

Although there are some previous research works regarding particle resuspension due to stepping, there is still a lack of knowledge about the physical concepts of the resuspension process. Besides, the effect of stepping features, especially the stepping time as a criterion for the walking speed, has not been assessed yet. In this research, the induced airflow and the resultant particle detachment due to the human stepping process were investigated numerically using the dynamic mesh approach. Based on the results, as the foot moves down towards the floor, tip vortices are induced and grow on the heel and toe. Besides, the surrounding air is ejected outwards from the sole and floor gap. During the upward motion of the foot, a strong gap flow, which is induced beneath the sole, pushes the surrounding air towards the centerline of the shoe, especially to its toe portion. Generally, particles are mainly resuspended in the downward motion and then entrained into the far-field airflow during the upward motion of the foot. The simulation results showed that locations close to the sole edges are the most susceptible zones for particles to be detached from the floor.

The effects of the main geometric features of the stepping process, including the stepping time and the shoe size on the resuspension and deposition rates of particles, were also studied. Accordingly, fast walking leads to a higher resuspension rate per footstep than less active, slower walking, mainly because of increased shear stress on the floor. Although the shoe size also affects the rate of particle resuspension, it is not as important as the stepping time. This study and its results provided a better understanding of the induced airflow and particle dispersion due to human activities such as walking. It may find practical applications in developing solutions to minimize their unfavorable effects.

References

[1] Kenney, S.M., Two Dimensional Particle Image Velocimetry Analysis of Flow Around a Stomping Mechanism, M.Sc. Thesis (2005), Clarkson University.

[2] Klepeis, N.E. et al. The National Human Activity Pattern Survey (NHAPS): A Resource For Assessing Exposure to Environmental Pollutants, J. Exposure Anal. Environ. Epidemiol., (2001) 11: 231-252.

[3] Rivas, I., Fussell, J.C., Kelly, F.J. and Querol, X., Indoor Sources of Air Pollutants, Indoor Air Pollution (2019), The Royal Society of Chemistry.

[4] Lewis, R.D., Ong, K.H., Emo, B., Kennedy, J., Kesavan, J., Elliot, M., Resuspension of House Dust and Allergens During Walking and Vacuum Cleaning, J. Occup. Environ. Hyg. (2018) 15: 235-245.

[5] Qian, J., Ferro, A.R., Resuspension of Dust Particles in a Chamber and Associated Environmental Factors, Aerosol Sci. Technol. (2008) 42: 566-578.

[6] Thatcher, T.L., Layton, D.W., Deposition, Resuspension, and Penetration of Particles within a Residence, Atmos. Environ. (1995) 29: 1487-1497.

[7] Nazaroff, W., Indoor Particle Dynamics, Indoor Air (2004) 14: 175-183.

[8] Khalifa, H.E., Elhadidi, B., Particle Levitation due to a Uniformly Descending Flat Object, Aerosol Sci. Technol. (2007) 41: 33-42.

[9] Kubota, Y., Hall, J.W., Higuchi, H., An Experimental Investigation of the Flowfield and Dust Resuspension due to Idealized Human Walking, J. Fluids Eng. (2009) 131: 081104.

[10] Zhang, X., Ahmadi, G., Qian, J., Ferro, A.R., Particle Detachment, Resuspension and Transport due to Human Walking in Indoor Environments, J. Adhes. Sci. Technol. (2008) 22: 591-621.

[11] Oberoi, R.C. et al., Human Induced Particle Resuspension in a Room, Aerosol Sci. Tech. (2010) 44: 216-229.

[12] Kubota, Y., Higuchi, H., Aerodynamic Particle Resuspension due to Human Foot and Model Foot Motions, Aerosol Sci. Technol. (2013) 47: 208-217.

[13] Goldasteh, I., Tian, Y.L., Ahmadi, G., Ferro, A.R., Human Induced Flow Field and Resultant Particle Resuspension and Transport during Gait Cycle, Build. Environ. (2014) 77: 101-09.

[14] Tian, Y., Sul, K., Qian, J., Mondal, S., Ferro, A.R., A Comparative Study of Walking-Induced Dust Resuspension Using a Consistent Test Mechanism, Indoor Air (2014) 24: 592-603.
[15] Qian, J., Peccia, J., Ferro, A.R., Walking-Induced Particle Resuspension in Indoor Environments, Atmos. Environ. (2014) 89: 464-481.
[16] Khare, P., Marr, L.C., Simulation of Vertical Concentration Gradient of Influenza Viruses in Dust Resuspended by Walking, Indoor Air (2014) 25: 428-440.
[17] Han, Z., Weng, W., Haung, Numerical And Experimental Investigation on the Dynamic Airflow of Human Movement in a Full-Scale Cabin, HVAC&R Research (2014) 20: 444-457.
[18] Benabed, A., Limam, K. Resuspension of Indoor Particles due to Human Foot Motion, Energy Procedia (2017) 139: 242–247.
[19] Lai, A.C.K., Tian, Y., Tsoi, J.Y.L., Ferro A.R., Experimental Study of the Effect of Shoes on Particle Resuspension from Indoor Flooring Materials, Build. Environ. (2017) 118: 251-258.
[20] Wang, B., Tang, Z., Li, Y., Cai, N., Hu, X., Experiments and Simulations of Human Walking-induced Particulate Matter Resuspension in Indoor Environments, J. Clean. Prod. (2021) 295: 126488.
[21] Zhang, L., Yao, M., Walking-induced Exposure of Biological Particles Simulated by a Children Robot with Different Shoes on Public Floors, Environ. Int. (2022) 158: 106935.
[22] Yakhot, V., Orszag, S.A., Thangam, S., Gatski, T.B., Speziale, C.G., Development of Turbulence Models for Shear Flows by a Double Expansion Technique, Phys of Fluids A (1992) 4: 1510-1520.
[23] Launder, B.E., Spalding, D.B., The Numerical Computation of Turbulent Flows, Comput. Meth. Appl. Mech. Eng. (1974) 3: 269-289.
[24] Chen, Q., Comparison of Different k-ε Models for Indoor Airflow Computations, Numer. Heat Transfer: Part B (1995) 28: 353-369.
[25] Ansys Fluent 12.1 User's Guide (2009), Ansys Inc.
[26] Patankar, S.V., Numerical Heat Transfer and Fluid Flow (1980), Taylor & Francis.
[27] Sajadi, B., Saidi, M.H., Ahmadi, G., Numerical Evaluation of the Operating Room Ventilation Performance: Ultra-Clean Ventilation (UCV) Systems, Sci. Iran. (2019) 26: 2394-2406.
[28] Johnson, K.L., Kendall, K., Roberts, A.D., Surface Energy and the Contact of Elastic Solids, Proc. R. Soc. London Ser. A (1971) 324: 301-313.
[29] Soltani, M., Ahmadi, G., On Particle Adhesion and Removal Mechanisms in Turbulent Flows, J. Adhes. Sci. Technol. (1994) 8: 763-785.
[30] Fuller, K.N.G., Tabor, D., The Effect of Surface Roughness on the Adhesion of Elastic Solids, Proc. R. Soc. London Ser. A (1975) 345: 327-340.
[31] Soltani, M., Ahmadi, G., Particle Detachment from Rough Surfaces in Turbulent Flows, J. Adhes. (1995) 51: 105-123.
[32] Greenwood, J.A., Williamson, J.B.P., Contact of Nominally Flat Surfaces, Proc. R. Soc. London Ser. A (1966) 295: 300-319.
[33] Fan, F.G., Ahmadi, G. A Sublayer Model for Turbulent Deposition of Particles in Vertical Ducts with Smooth and Rough Surfaces, J. Aerosol Sci. (1993) 24: 45-64.
[34] Qian, J., Ferro, A.R., Fowler, K.R. Estimating the Resuspension Rate and Resident Time of Indoor Particles, J. Air & Waste Manage. Assoc. (2008) 58: 502-516.
[35] Sajadi, B., Saidi, M.H., Ahmadi, G., Kenney, S.M., Taylor, J., On the Induced Airflow and Particle Resuspension due to a Falling Disk, Particul. Sci. Technol. (2013) 31: 190-198.
[36] Leweke, T., Thompson, M.C., Hourigan, K., Vortex Dynamics Associated with the Collision of a Sphere with a Wall, Phys. Fluids (2004) 16:L74-L77.